The relationship between shallow thermal circulation regimes and cumulonimbus clouds along the northeastern Adriatic coast

Karmen Babić[1], Petra Mikuš[2] and Maja Telišman Prtenjak[1]

[1] University of Zagreb, Faculty of Science, Department of Geophysics,
Andrija Mohorovičić Geophysical Institute, Zagreb, Croatia

[2] Meteorological and Hydrological Service of Croatia, Zagreb, Croatia

The aim of this study is to determine the relationship between the occurrence of a sea breeze (SB) and cumulonimbus (Cb) clouds over the Istrian Peninsula. For this purpose, available standard surface measurements, i.e., the near-surface wind, the air and sea surface temperatures and cloudiness at two stations (Pula-Airport and Pazin), and satellite images were analyzed. The study was performed during the summer months (from June to September) for the years 1997–2006. The analysis showed that the Cb development was typically associated with certain meteorological conditions. These conditions were as follows: (i) SB speed at Pula-Airport in the range of 3–5 m s^{-1}, (ii) maximum temperature difference between sea and land near Pula-Airport around 4 °C, and (iii) maximum air temperature in Pazin in the range of 25 to 31 °C. On average, during the days with simultaneous development of SB and Cb clouds, the land breeze was weaker and the air temperature was higher than on other analyzed days. Diurnal cloud evolution showed that Cb clouds usually develop (above Pazin) between 13 and 14 h of Central European Time (CET). Cumulus clouds, as indicators of the SB inland penetration, preceded the Cb development. Satellite images for 2000–2006 obtained by the geostationary satellites Meteosat 7 and 8 were investigated, and a spatial distribution and a temporal development of 30 chosen Cb events were detected. Two characteristic regions of the Cb origin were noted: the northern and southeastern parts of the Istrian Peninsula. The Cb clouds usually formed between 11 and 13 CET, lasting in general from 3 to 5 hours and disintegrating between 15 and 17 CET.

Keywords: sea/land breeze, Istria, convergence zone, satellite images, sea breeze index

1. Introduction

Much of the world's population (according to some estimates, >50%, e.g., http://climatelab.org/Coastal_Development) lives in coastal areas under the atmospheric thermal circulation influence. Research conducted in last several

decades (e.g., Estoque, 1962; Atkinson, 1981; Simpson, 1994; Miller et al., 2003) has revealed the basic mechanisms of the thermal circulation formation. It is based on the temperature (and consequently pressure) difference between the land and sea and is qualitatively comparable with the emergence of the general circulation of the atmosphere on a large scale. However, thermal circulation is strongly modified by specifics of the topography, which have been shown in many previous studies (Pielke, 1974; Grisogono et al., 1998; Miller et al., 2003; Nitis et al., 2005; Prtenjak et al., 2006).

Shallow thermally-induced flow is usually associated with a particular cloud type (Pielke and Mahrer, 1978; Sano and Tsuboki, 2006). If there is a merging of two (or more) coastal circulations, it will cause the formation of a convergence zone in which updraft is significantly increased (Dailey and Fovell, 1999). In these converging areas, cumulonimbus (Cb) clouds can easily develop, as in Florida (Pielke, 1974; Pielke and Mahrer, 1978; Nicholls et al., 1991; Pielke, 1991). Pielke (1974) was among the first who showed, using three-dimensional (3D) numerical mesoscale model simulations that the position of a storm along the east coast of Florida is under the control of the position and motion of the sea breeze (SB). However, due to the relatively weak SB convergence zone, Cb clouds may be relatively small and short lived (Wilson and Megehardt, 1997). Yuter and Houze (1995) examined the kinematics and microphysical evolution of Cb clouds in Florida during SB event with weak vertical wind shear. Based on the high-resolution radar data, they revealed the 3D structure and evolution of the multicellular squall lines showing (among other things) that updrafts tended to be located near the leading edge of the storm. In Japan, over complex terrain including flat and mountainous parts of the coast, SB and valley wind above the Kanto plain appear at the same time (Kondo, 1990; Iwasaki, 2004). Two maxima of convective activity were found, the daytime (10–14 h of local time) and evening one (18–22 h of local time), that coincided with the maxima of precipitable water. The daytime maximum of precipitable water originated from the transport of moisture that was associated with valley circulation from the early morning until noon. The evening maximum was caused by the moisture convergence because of the »extended SB« from 15 h local time until late evening. An increase of precipitable water during both intervals acted to enhance the instability resulting in Cb cloud formations. During the summer, using radar measurements, Sano and Tsuboki (2006) simultaneously observed developments of Cb clouds, valley wind above the mountain areas and SB at the coast. They concluded that the upward current due to local valley winds is increased by upward movement at the SB front and by the convergence behind it. As a result, Cb clouds form over the hills. Over the Iberian Mediterranean zone, Azorín-Molina et al. (2009) statistically analyzed the impact of SB on cloud types in the convective internal boundary layer and in the SB convergence zone. The study examined the southeast of the Iberian Peninsula over a 6 year period (2000–2005). The results confirm that SB causes a higher frequency of low clouds (stratus)

within the convective internal boundary layer and convective clouds (cumulus) near the SB fronts. Stratus clouds occur most often in the morning during June and August (with an average monthly frequency of 16%) as the moist morning sea air of the SB contributes to the formation of low cloud cover. Cumulus clouds are common from July to September in the early afternoon (13 UTC) with an average monthly frequency of 30%. The SB acts as a driving force for the formation of storm clouds in the SB convergence zone. This study showed that the mean monthly frequency of Cb clouds and the SB is up to 4%. Cb clouds occur earlier in the spring and autumn (at 13 UTC, disappear at 18 UTC). During the summer maximum in July, Cb clouds develop later during the day and reach daily maximum at 18 UTC. Despite a variety of studies investigating the relationship between SB and cloud types, the existed conclusions about their relationship cannot be simply applied to the unexplored topographic complex region.

The northeastern Adriatic coast (Fig. 1), which is a good example of a very complex coastline in the central part of the Mediterranean, was recently a target of research regarding the sea/land breeze phenomenon. Existed studies (Nitis et al., 2005; Prtenjak et al., 2006, Klaić et al., 2009; Prtenjak et al., 2010) revealed some specific features in the mesoscale wind field within the atmospheric boundary layer. It was noted that the convergence zone is formed along Istria as a result of unifying several thermal circulations during the day.
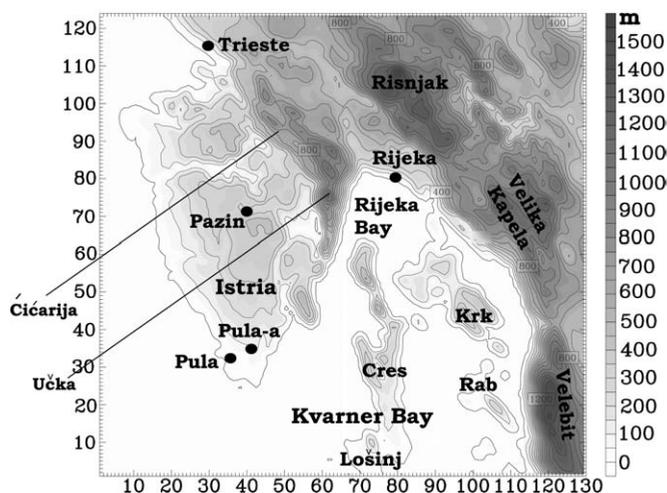

Figure 1. Topographic map of the northeastern Adriatic coast with the positions of the measuring sites; hourly meteorological measurements at the Pula Airport (Pula-a) and Pazin. Topography contours are given for every 100 m between 0 and 1700 m. The highest points in Istria are the mountain massifs of Ćićarija (~ 1100 m a.s.l.) and Učka (~ 1400 m a.s.l.). Kvarner Bay encompasses, besides the smaller Rijeka Bay, the islands of Krk (the largest), Cres, Lošinj and Rab. East of Kvarner Bay, high mountains such as Risnjak (~ 1500 m a.s.l.), including Velika Kapela (~ 1500 m a.s.l.) and Velebit (~ 1600 m a.s.l.) are located.

On average, along the northeastern Adriatic coast that represents the area with the highest frequency of thunder (Makjanić, 1958) and lightning (Mikuš et al., 2012) in Croatia, the SB occurs every other summer day (e.g., Prtenjak and Grisogono, 2007).

Previous studies of the SB along the northeastern Adriatic coast were primarily focused on the wind characteristics, while the relationship between SB and Cb clouds was not investigated. Considering that the airport is located at the tip of Istrian Peninsula and that convective clouds, in particular the Cb clouds, are known for their strong vertical unsteady flow causing major problems in air traffic forecast, the determination of SB-Cb relationship above Istria would be very useful. Therefore, the goal of this study is to determine the relationship between the SB and summer convective Cb cloud in Istria. This analysis was conducted using available surface and remote, primarily satellite, measurements and thus fills an important gap in the understanding of weather patterns in this area.

2. Study area, data and methods

2.1. Study area

The northeastern Adriatic coast covers Istria (a large peninsula surrounded by sea on three sides), a number of islands in the Kvarner bay and Rijeka (a city and a port placed south of the Risnjak mountain range; 1500 m high). Southeastward of Istria are the Velika Kapela and Velebit mountains (Fig. 1). Istria is divided into three geographical regions: the mountainous northern edge (limestone mountains of Trieste Karst and Ćićarija; ~1100 m high), the lower region (where the Pula-Airport is located) and open low limestone plateau (where station Pazin is located). The highest peak of the peninsula is in the east: Učka of ~1400 m above sea level (a.s.l.). The Istrian Peninsula belongs to the general Mediterranean type of climate, which is often influenced by the Azores anticyclone during the summer. In such conditions, when synoptic forcing was weak, formation of local thermal circulations frequently occurred (e.g., Prtenjak and Grisogono, 2007).

2.2. Surface measurements

We focus on the summer months, when the SB development is frequent (e.g., Prtenjak and Grisogono, 2007), analyzing surface measurements for two meteorological stations, the Pula-Airport and Pazin (Fig. 1). Collected data included hourly wind, sea surface temperature (SST) and 2-m air temperature over land. Precipitation and cloudiness are observed from June to September during a 10-year period (1997–2006). The cloudiness (in tenths), cloud types (low, medium and high) and precipitation data were collected only for the Pazin site for the two limited time intervals, from 5–14 h of Central European

Table 1. Geographical features of latitude (φ), longitude (λ), altitude (H), station distance from the shore (D) and the number of analyzed days (N) used in the study during the summer (June-September) over the period 1997–2006. Meteorological variables (MV) used in analysis are: wind speed (V, m s⁻¹), air temperature (T, °C), cloud cover (N, 1/10) and precipitation (P, mm).

Station	φ	λ	H (m)	D (km)	N	MV
Pula-Airport	44° 54' N	13° 55' E	63	10	1097	V, T
Pazin	45° 14' N	13° 56' E	291	25	1220	V, T, N, P

Time (CET) and during 19–21 CET. SST was measured at the coastal site Pula, 10 km away from the Pula-Airport station (Fig. 1). Tab. 1 shows the particular specifications of the stations and the total number of days analyzed during the whole study period.

In previous studies of coastal circulation climatology (Lukšić, 1989; Borne et al., 1998; Furberg et al., 2002; Prtenjak and Grisogono, 2007; Azorin-Molina et al., 2011), several criteria for the determination of days dominated by the SB were proposed. Here we used slightly modified criteria given by Prtenjak and Grisogono (2007). The determination of SB days (set A) at the Pula-Airport station was conducted through surface measurements of wind speed and direction and the difference between air temperature over land and SST. The modification we employed was in the temperature criterion, which is here defined as $\Delta T = t_{land} - SST > 0$ °C, somewhat similar as in Furberg et al. (2002) and Azorin-Molina et al. (2011). The maximum air temperature over land (between 12 and 16 CET) is denoted as t_{land}, and SST is measured at 14 CET in Pula. The chosen data set (A) contains 563 days with SB at the Pula-Airport (Tab. 2).

The main criterion for the Cb day in Pazin was the presence of daytime Cb cloud between 11 and 21 CET during the same investigated period (June to September, 1997–2006). Nighttime and early morning Cb cloud occurrences are associated with frontal passages rather than with the SB over the penin-

Table 2. The number and frequency of SB days at the Pula-Airport (set A), the number of days with Cb clouds in Pazin (set B) and the number of days with SB and Cb clouds (set C) from June to September 1997–2006.

Pula-Airport	Number of SB days = set (A)	563
	SB frequency	51%
Pazin	Number of days with Cb clouds in Pazin = set (B)	99
	Frequency of the daytime Cb during warm months	8.4%
Pula-Airport ∩ Pazin	Number of days with SB and Cb clouds = set (C)	51
	Frequency of the daytime Cb during SB events at the coast	9.1%

sula and are therefore excluded from our analyses. Selecting data in this way has led to 99 days (set B). Unfortunately, due to some technical difficulties in Pazin, the certain number of maxima daily air temperature measurements in 2002 is missing.

Based on previous (A) and (B) datasets, we obtained three new datasets:

• Data set (C) (= set A ∩ set B), which represents both when the SB is prevailing at the Pula-Airport and a Cb cloud is observed in Pazin. The set (C) has 51 days, and the relative frequency of the cloud genus is calculated for each term of observation.

• Data set (D) (= set A – set C) consists of those days when the SB is prevailing at the Pula-Airport and Cb cloud is not recorded in Pazin.

• Data set (E) (= set B – set C) consists of those days when occurrence of Cb cloud is recorded in Pazin, but there is no SB at the Pula-Airport.

2.3. Satellite measurements

The time and place of Cb origin, time of its disappearance, space coverage and Cb cloud evolution in time were traced by satellite images. Satellite images were available only for the period of 2000–2006; therefore, 30 days of set (C) (i.e., 58% of the overall selected days with Cb development) were recorded from space. Satellite images were obtained from the geostationary satellite in three spectral channels VIS, IR and WV in the period 2000–2003 from Meteosat 7 and in 2004–2006 from Meteosat 8. A combined channel CH139 (VIS + IR) was used for better visualization of certain phenomena in the Earth's atmosphere.

3. Results

3.1. Surface measurements

Tab. 2 shows some initial characteristics of the selected data sets. The frequency of SB days is around 51%, which agrees with the findings of Prtenjak and Grisogono (2007) despite having somewhat modified criteria. Furthermore, we found a total of 99 daytime Cb cloud cases recorded in 8.4% of all days analyzed. Besides this, the total number of days in set (C) contains 51.5% of set (B) or every other Cb day in Pazin. This finding suggests that in a relatively large number of cases, reported occurrence of Cb clouds, could be linked with the development of coastal circulation on the shore. According to data set (C), the Cb clouds occurred in 9.1% of all days with the SB phenomenon. The largest numbers of combined cases were found in 1999 and 2003 (not shown) with significant year-to-year variability and without any significant trend.

Mean monthly variability of data set (A) in Fig. 2 showed that the SB is very frequent from June to August resulting in 55–60% of all the analyzed summer days, with significant decreasing in September. Furthermore, the largest frequency of daytime Cb events (set B) was recorded in July (exceeding
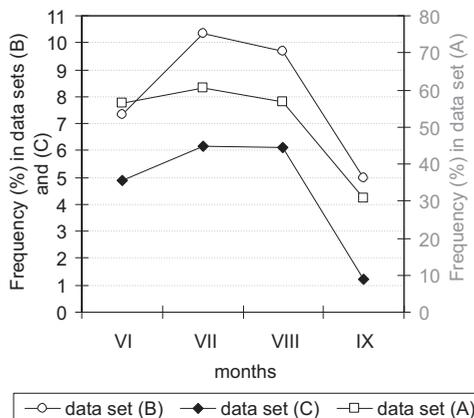
Figure 2. The monthly frequency (%) of SLB days (squares, data set A) at the Pula-Airport station and the monthly frequency (%) of Cb days in Pazin without (circles, data set B) and with (rhombs, data set C) simultaneous detection of SB at the Pula-Airport from June to September 1997–2006.

10% of all summer days in particular month) and coincides with the largest overall convective activity (Mikuš et al., 2012). Data set (C) shows similar monthly behavior; the majority of such combined cases is in July and August (in ~6% of all summer days), while they are the rarest in September. Interestingly, the mean monthly frequency higher than 6% obtained here is larger of 4% what reported Azorín-Molina et al. (2009) for the southeastern coast of Spain. The difference is also in the preferable summer month which is July in Istria versus September in Spain.

The climatological relationship between the SB and the occurrence of Cb clouds was further analyzed for selected datasets. During the development of Cb clouds and presence of SB at the Pula-Airport, the most frequent maximum daily temperature in Pazin is 26 °C (Fig. 3a). If the maximum temperature is less than 24 °C, the Cb clouds do not develop. For temperatures higher than 31 °C, the Cb-occurrence is relatively rare. Furthermore, Cb clouds in Pazin usually form when the maximum ΔT (at the Pula-Airport) is around 4 °C (Fig. 3b) corresponding to the most favorable ΔT for the SB development and its maximum speeds along the Adriatic coast (Prtenjak and Grisogono, 2007). According to the linear relationship between the maximum air temperature in Pazin and the maxima ΔT at the Pula-Airport, the correlation coefficient is high for both sets, that is, for set (C) $r = 0.78$ and for set (D) $r = 0.81$; Fig. 3c. Both results are statistically significant at a significance level $\alpha = 0.05$. Therefore, the highest temperature differences are associated with very high maximum air temperatures in Pazin when the development of Cb clouds is very sporadic (e.g., for $\Delta T > 5$ °C and t_{max} (Pazin) > 31 °C, there were only 6 cases). Concerning the intensity of the onshore flow (Fig. 3d), the Cb clouds are usually observed when the wind speed of SB at the Pula-Airport is between 3 and 5 m s^{-1}.
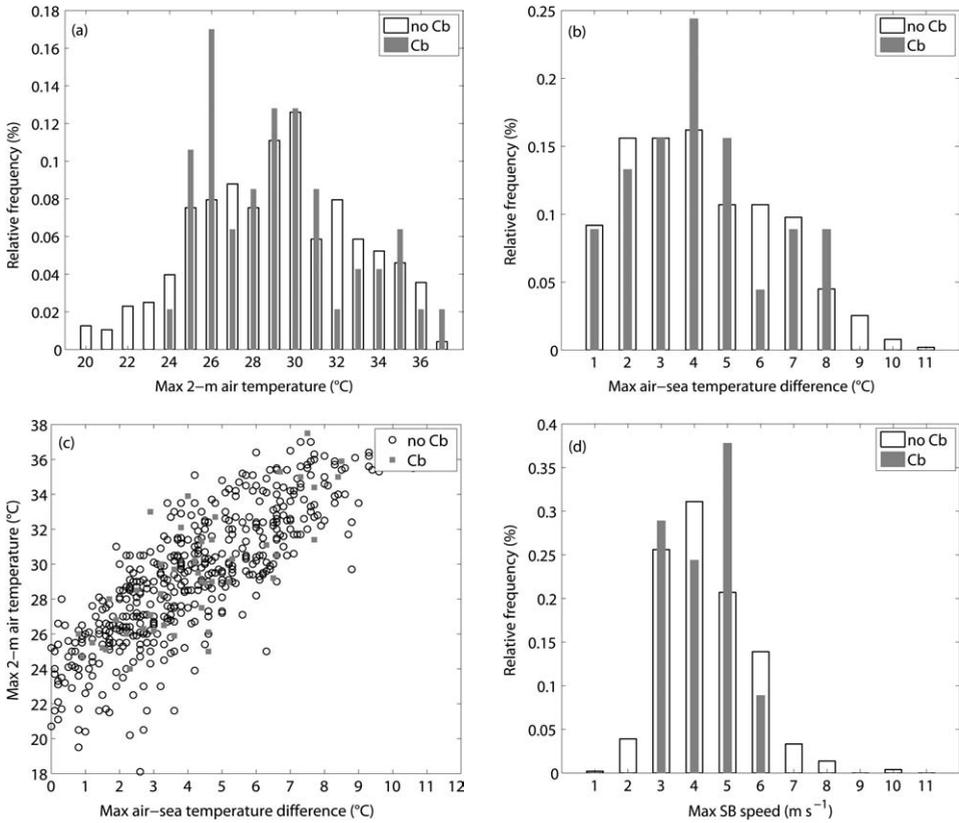
Figure 3. Relative frequency of (a) the maximum daily temperature in Pazin and (b) maximum ΔT at the Pula-Airport for set (C) (grey) and set (D) (white). Presentation is divided into Cb and no Cb events in order to analyze a climatological relationship between the SB and the occurrence of Cb clouds. (c) The maximum ΔT at the Pula-Airport and maximum daily temperature in Pazin for the set (C) (black) and set (D) (grey). The correlation coefficient between these two values is 0.78. (d) The relative frequency of the maximal SB velocities for a set (C) (grey) and set (D) (white).

There are several reasons for the preferable range of maximal air temperatures. The direct connection is that the occurrence of Cb clouds will reduce radiant solar energy and long-wave radiation and thus prevent further increases in air temperature. There is also a negative feedback between the SB wind speeds and the maximum daily temperature in Pazin. The possible origin of such patterns comes from the SB inland advection of the colder marine air deep over peninsula (over 30 km). SB speeds at the Pula-Airport between 3 and 5 m s^{-1} and the formation of well-known SB convergence zone (e.g., Prtenjak et al., 2006) along the peninsula are associated with more intense updrafts. Higher vertical velocities create favorable conditions for the development of Cb clouds (e.g., Dailey and Fovell, 1999; Yuter and Houze, 1995). Thus,
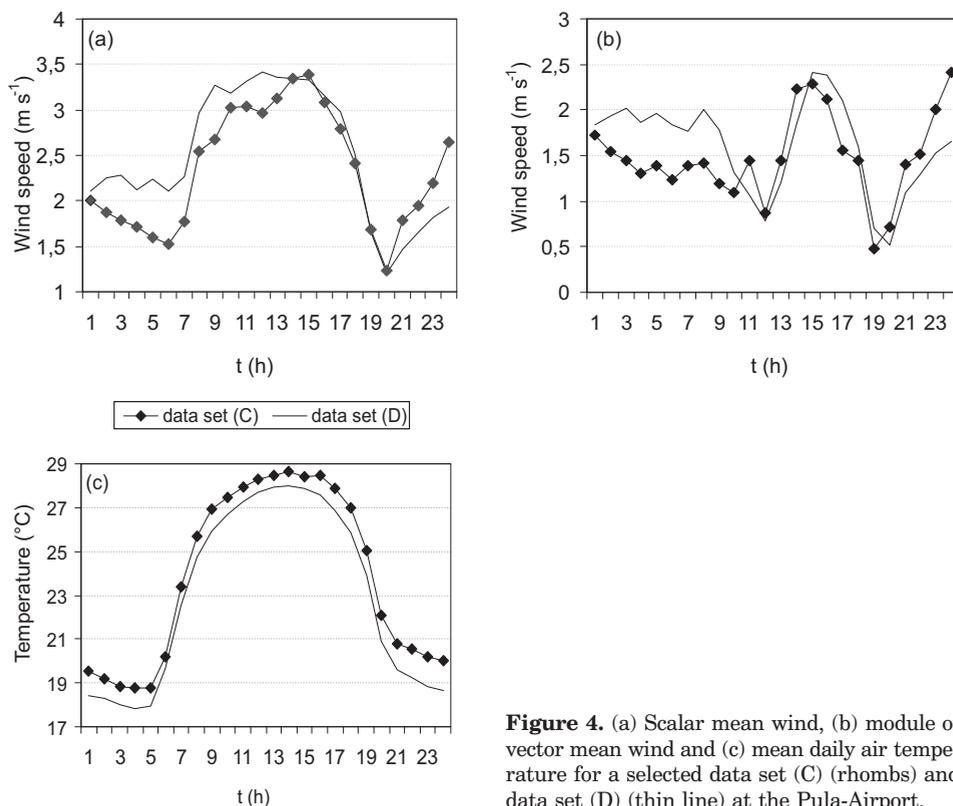
Figure 4. (a) Scalar mean wind, (b) module of vector mean wind and (c) mean daily air temperature for a selected data set (C) (rhombs) and data set (D) (thin line) at the Pula-Airport.

higher-speed SBs (i.e., > 6 m s^{-1}, Fig. 3d), ΔT > 6 °C (Fig. 3c) associated with t_{max} (Pazin) > 32 °C represent less well-disposed meteorological conditions for the convective activity above the central part of Istria. It could be that the Cb development occurred farther north or west of Pazin (due to higher onshore speeds), and therefore, it is not visible by surface network observations. Alternately, very weak coastal winds cannot contribute significantly to the formation of the convergence zone (if it happens at all) because they are too weak to lead to any significant vertical lift of air and consequently development of Cb clouds. However, a more accurate explanation for this relationship between meteorological quantities can be obtained using a numerical mesoscale model.

We also compared averaged daily courses of wind (scalar mean, vector mean), air temperature and ΔT for different data sets for the Pula-Airport (Fig. 4) and Pazin (Fig. 5). At the Pula-Airport, the comparison of scalar and vector mean wind shows that in the case of Cb generation over central part of peninsula, there was a slightly weaker land breeze on the coast prior to the SB (Figs. 4a, b). A situation in which there was no significant transfer of warm air

from the interior to the coast is favorable for increased local instability through-out the day and for the development of Cb clouds. At the same time, inland wind speeds were somewhat higher in cases where Cb was developing (Fig. 5a), when compared to the non SB days.

On average, the days when Cb was observed had warmer nights, both on the coast (Fig. 4c) and inland (Fig. 5b). Daily mean temperatures for Pazin (Fig. 5b) show that for set (C) the minimum temperatures are about 2 °C high-er than those in set (D). The average daily maximum is about 28 °C in both sets, and the Cb development is seen in the decrease in air temperature between 12 and 17 CET. For data set (E), the daily air temperature range is much lower and the mean maximum air temperature does not exceed 22 °C. This finding indicates that development of Cb in Pazin is a result of cooling on a larger scale, probably due to the passage of a cold front. This finding is in accordance with the total cloud cover, which is not less than 6/10 for set (E) (Fig. 5c) and the rainfall which prevails at night. For set (D), there is a daily cloud cover maximum (10/10) and the average precipitation is less than 3 mm. Similar behavior is seen for set (C), although the daily maximum of total cloud cover in
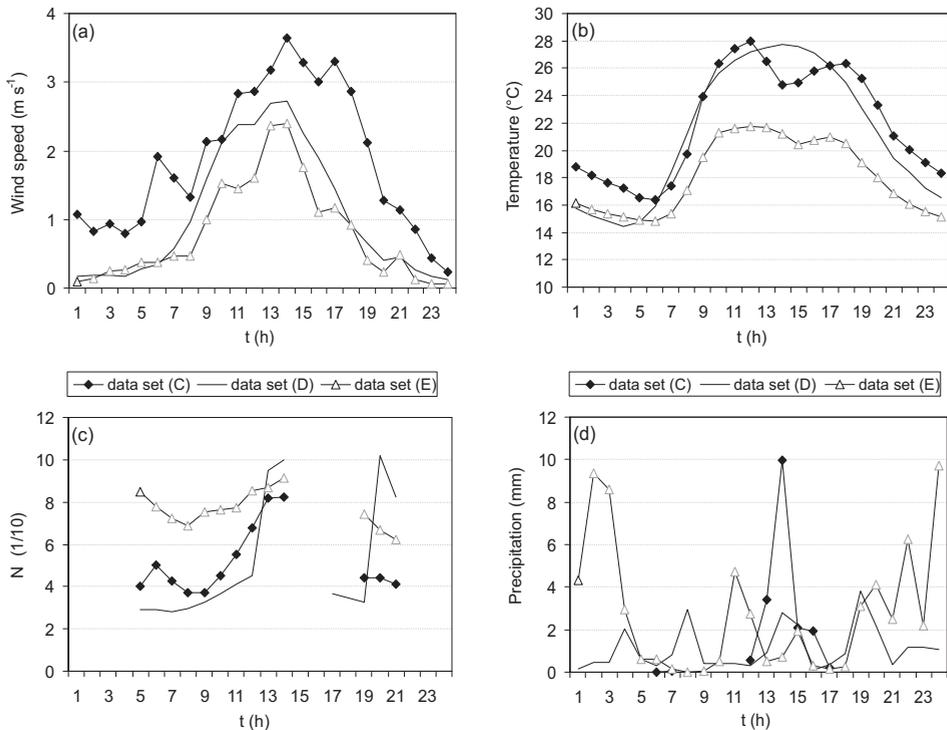

Figure 5. (a) Scalar mean wind, (b) mean daily cycle of 2-m air temperature, (c) mean daily cycle of cloudiness in Pazin and (d) mean daily cycle of precipitation in Pazin for data set (C) (rhombs), data set (D) (thin line) and data set (E) (triangles).
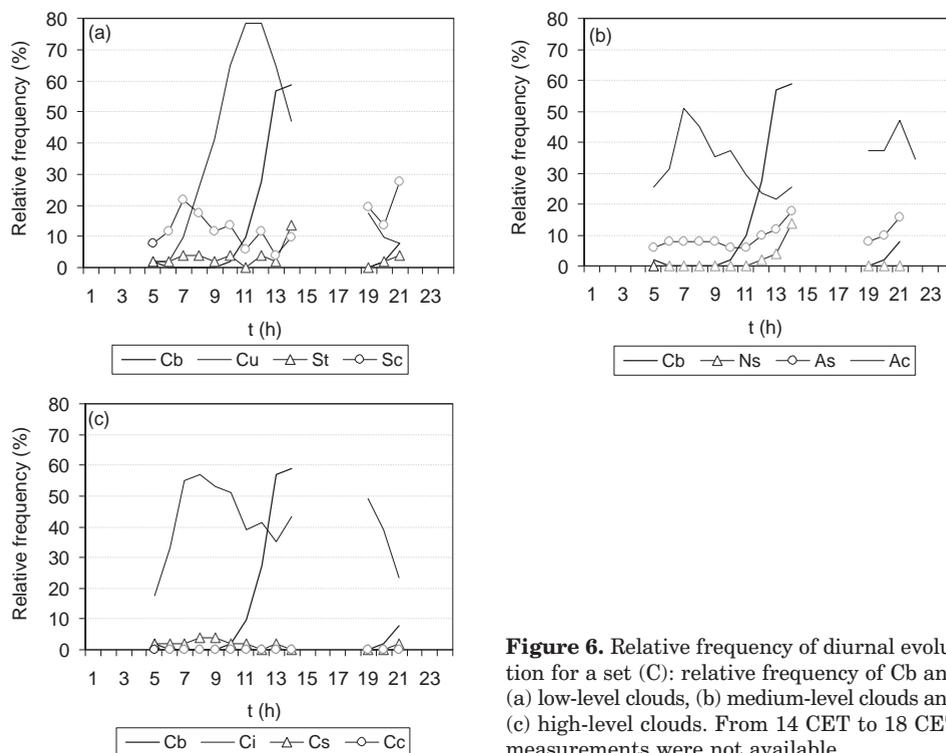
Figure 6. Relative frequency of diurnal evolution for a set (C): relative frequency of Cb and (a) low-level clouds, (b) medium-level clouds and (c) high-level clouds. From 14 CET to 18 CET measurements were not available.

Pazin is associated with the maximum precipitation of about 10 mm, which is found between 13 and 15 CET.

Figure 6 summarizes the frequency distribution of cloud genera for the ten categories of data set (C) during the period studied. At 14 CET, the frequency of Cb is the highest, nearly 60% (Fig. 6a). The development of Cb usually occurs between 12 and 14 CET. Cumulus clouds are formed prior to Cb development. They start to develop in the early morning and have the highest relative frequency between 10 and 13 CET. In the hours that precede the Cb development, cumulus clouds have relative frequency of almost 80%. Stratus clouds have a low relative frequency throughout the day, as opposed to in southeast Spain (Azorin-Molina et al., 2009), where relatively high stratus formation has been observed in the morning hours. Among mid-level clouds, the altocumulus clouds are the most frequently observed and have average relative frequency of 35% (Fig. 6b). Cirrus clouds are the most common high--level clouds (Fig. 6c). For days in which the Cb clouds were observed in Pazin, some types of clouds were not monitored (cirrocumulus) or they have a relatively low frequency (stratus, nimbostratus, altostratus, cirrostratus). Note that fluffy clouds, such as altocumulus, stratocumulus, cumulus clouds and Cb clouds, indicate the existence of atmospheric convection.

3.2. Sea breeze index

According to the previously mentioned results, we can estimate the SB index (ε) for the past occurrence of SB. Many authors used this approach to forecast and/or identify the SB and lake breeze, e.g., Biggs and Graves (1962), Simpson (1994), Laird et al. (2001). Such a method is based on the ratio of the inertial force (given by the wind speed) and buoyancy force (given by the air-sea temperature difference). Here, the technique of Biggs and Graves (1962) and Laird et al. (2001) was employed. The main goal is to find specific values of the SB index that give a range of values of the likelihood of the simultaneous SB and Cb appearance.

At the Pula-Airport (10 km away from the coast), the quantities for the ε estimation for each day within data set (C) include (i) ΔT (°C) and (ii) the average daytime (10–16 CET) wind speed V (m s^{-1}). It is defined as

$$\varepsilon = \frac{V^2}{C_p \Delta T},$$

(1)

where C_p is the specific heat of dry air at constant pressure (1003 J kg^{-1} K^{-1}). Here, the mixture of cgs and SI units in C_p is retained (like in Laird et al., 2001)

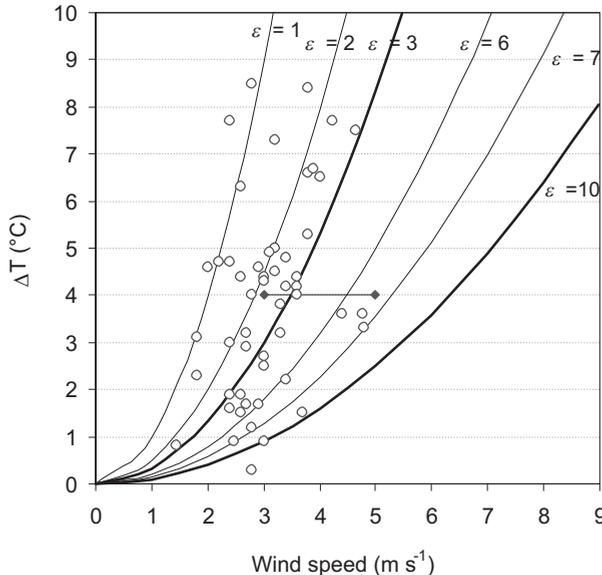**Figure 7.** SB index (ε) calculated by the Eq. (1) (see text) for the Pula-Airport data using data set (C). The index represents the ratio between the mean daytime (10–16 CET) wind speed (m s^{-1}) and maximum air-sea temperature difference ΔT (°C). Curves denote values of ε = 1, 2, 3, 6, 7 and 10 where black ε curves correspond to the Biggs and Graves (1962) critical values with high accuracy in SB predicting. Two rhombs represent ε values (in the range of 2–7) for the most favorable combined SB and Cb occurrence.

Table 3. Available days in the set (C): development, disappearance and duration of Cb and area of Cb development. The mean starting and decaying times as well as the mean duration are in the brackets.

Number of analyzed cases	Area of generation	Starting time (CET) (mean, CET)	Ending time (CET) (mean, CET)	Duration (hours) (mean, h)
22	SE Istria	from 10 to 13 (12)	from 14 to 17 (15.5)	from 2 to 6 (3.5)
7	N Istria	from 11 to 12 (11.6)	from 15 to 17 (15.6)	from 3 to 5 (4)

because we want to compare ε values with prior studies. Furthermore, average daytime wind speed, as in Biggs and Graves (1962), is used rather than average daytime shore-perpendicular wind speed, as in Laird et al. (2001). Diurnal wind above Pula-Airport is highly influenced by the Istrian convergence zone (Prtenjak et al., 2008) as the result of the merging of two SB systems from the opposite coastlines making the shore-perpendicular wind component approach very inapplicable here.

Figure 7 shows calculated ε (Eq. 1) for the Pula-Airport station data using data set (C). Black curves ($\varepsilon = 3$ and $\varepsilon = 10$) correspond to the Biggs and Graves (1962) critical values representing ε-range of high accuracy in the SB prediction. About 40% of the calculated indices, ε, are in the range of 3 to 10, the method again underestimates the number of reported SB events as argued in Laird et al. (2001). Biggs and Graves (1962) stated that the critical values cannot be simply applied without modification for other locations. However, the aim here was not to find thresholds concerning the SB detection but to provide the range as well as the most optional values for the coincidental SB and Cb events. Therefore, the results revealed that the suitable meteorological condition leading to the SB and Cb development would be for ε between 1 and 10 with most desirable value between 2 and 7 (rhombi in Fig. 7).

3.3. Satellite images

Based on satellite images, there are two characteristic locations of Cb origin, the southeastern and mountainous northern parts of Istria. Cb clouds occur in the southeastern part of Istria in 22 of 30 available cases, while Cb occurs in the northern part of Istria in 7 cases (Table 3). The Cb mostly developed between 11 and 13 CET, and it usually disappeared between 15–17 CET typically lasting 3–5 hours. The summer Cb occurrence in this region is earlier than in southeastern Spain (Azorín-Molina et al., 2009).

Figure 8 shows the spatial coverage and development time of Cb clouds, which originated in southeastern Istria on 8 August 2006. On that day, the SB was recorded in both Pula and Rijeka (for sites see Fig. 1). Until 12 CET nearly clear sky above Istria were disturbed by Cb development above the
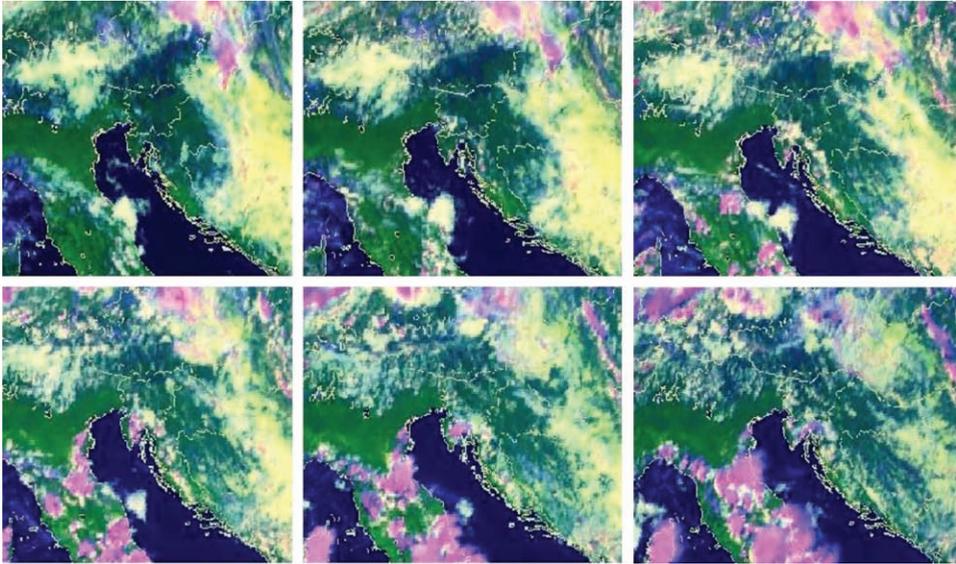
Figure 8. Satellite images on 8 August 2006, from left to right, every hour from 10 CET to 15 CET in the combined (VIS + IR; channel CH139) channel received from Meteosat 8. Example of the Cb development above the southeastern part of Istria. The pink color represents convective clouds, yellow and white colors are other types of cloud, green is land and blue is sea.
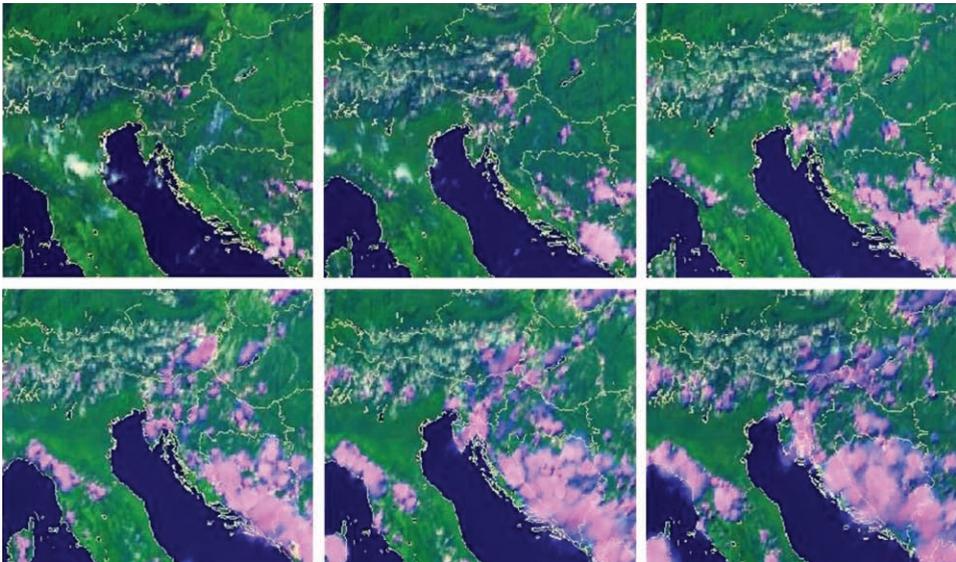

Figure 9. Satellite images on 25 July 2006, from left to right, every hour from 10 CET to 15 CET in the combined (VIS + IR; channel CH139) channel received from Meteosat 8. An example of the creation of Cb above the northern part of Istria. The pink color represents the convective clouds, yellow and white colors are other types of cloud, green is the land and blue is the sea.

southeastern part of Istria. As time progressed, the Cb cloud grew and covered much of the interior by 13 CET, while the sky is clear on the west coast of Istria. Between 14 and 15 CET, the clouds gradually dissolve and, Cb disbanded the greater part of central Istria at 15 CET. Figure 9 shows the development of another case of Cb, which originated in northern Istria (25 July 2006, from 10 to 15 CET). At 12 CET, the Cb cloud was over the northern part of Istria, while the sky was clear prior to the occurrence over the whole Istria. In time, the Cb cloud developed more and covered much of the interior and northern part of Istria. At 15 CET, the Cb vanishes, and the sky is predominantly clear almost over the whole of Istria. Throughout our data, one date was exceptional due to the specific location of the Cb's origin. On 21 August 2001 at 11 CET, two separate Cb clouds began to develop. One developed in the northern part and another in the southeastern part of Istria (not shown). Satellite images at 10 CET showed that the sky above Istria was clear; thus, we conclude that the Cb clouds, which started to develop, were not part of some front but were closely linked to local convection. This hypothesis is supported by their formation and duration. After some time, two separate Cb's were combined. On the satellite image at 12 CET, they can be seen as one Cb covering much of the interior of Istria, while the west coast had clear sky. Around 14 CET, the Cb was slowly dissolving, and the sky is relatively clear at 15 CET above Istria.

4. Conclusions

In this study, we attempted to determine the relationship between two phenomena: the sea breeze (SB) at the coastal stations and cumulonimbus (Cb) cloud in Istria. The data that we analyzed comprise hourly wind data, 2-m air temperature over land, sea surface temperature (SST), precipitation and cloud cover. The analysis was performed for the summer months (June–September) over a 10-year period (1997–2006). The data were collected at Pula for SST, the Pula-Airport for the (SB) detection and Pazin for the Cb cloud detection. The data set that includes the occurrence of both phenomena (SB and Cb clouds) was further analyzed by means of satellite images.

During all summer days, the frequency of the SB above the tip of Istria is 51% and the frequency of daytime (11–21 CET) Cb above the interior of peninsula is 8.4%, respectively. In 51% of daytime Cb days, SB develops along the coast.

The largest number of days with the simultaneous appearance of both features is in July that coincides with analyses of convection activity above the North Adriatic (Mikuš et al., 2012). The results have revealed the most optimal conditions for the Cb clouds generation. The Cb clouds often develop for the maximum 2-m air temperatures in Pazin in the range of 25 to 31 °C. If the maximum air temperature is less than 23 °C, or higher than 32 °C, the ap-

pearance of Cb clouds is rare. Furthermore, we identified a linear relationship between the maximum daily temperature in Pazin and the maximum land-sea temperature difference (ΔT) at the Pula-Airport. The Cb usually develops when (i) the maximum temperature in Pazin is between 25 and 31 °C, (ii) ΔT is in the range of 3 and 5 °C and when (iii) the maximum SB speed is between 3 and 5 m s^{-1}. A weak SB indicates a small inland penetration of the marine colder air, presumably a weak SB front, and consequently weak vertical updraft, and thus, no Cb development. However, the high speed of the onshore flow also precludes the development of Cb clouds over Istria. The results showed that prior to the development of Cb over the peninsula and the SB at the coast, higher nighttime air temperatures over the land and weaker land breeze occurred. Inspection of diurnal cloud evolution showed that the occurrence of Cb is frequently followed by some cloud genera, while some do not appear or are represented by small relative frequencies. The most frequent are cumulus clouds between 10 and 13 CET with a relative frequency greater than 70%. Altocumulus and cirrus usually occurred as well, and sporadic stratiform clouds were rather rare. Two specific areas of Cb generation were revealed, one at the southeastern part and another at the northern mountainous region of Istria. Cb starts to develop in the late morning or around noon and disappears around 15–16 CET with the duration between 3 and 5 hours.

References

Atkinson, J. E. (1981): *Meso-scale atmospheric circulations*. Academic Press, London, 494 pp.

Azorin-Molina, C., Sanchez-Lorenzo, A. and Calbo, J. (2009): A climatological study of sea breeze clouds in the southeast of the Iberian Peninsula (Alicante, Spain), *Atmosfera*, **22**, 33–49.

Azorin-Molina, C., Chen, D. L., Tijm, S. and Baldi, M. (2011): A multi-year study of sea breezes in a Mediterranean coastal site: Alicante (Spain), *Int. J. Climatol.*, **31**, 468–486.

Biggs, W. G. and Graves, M. E. (1962): A lake breeze index, *J. Appl. Meteorol.*, **1**, 474–480. DOI: 10.1175/1520-0450(1962)001<0474:ALBI>2.0.CO;2

Borne, K., Chen, D. and Nunez, M. (1998): A method for finding sea breeze days under stable synoptic conditions and its application to the Swedish west coast, *Int. J. Climatol.*, **18**, 901–914.

Dailey, P. S. and Fovell, R. G. (1999): Numerical simulation of the interaction between the sea-breeze front and horizontal convective rolls. Part I: Offshore ambient flow, *Mon. Wea. Rev*., **127**, 858–878.

Estoque, M. A. (1962): The sea breeze as a function of the prevailing synoptic situation, *J. Atmos. Sci.*, **19**, 244–250.

Furberg, M., Steyn, D. G. and Baldi, M. (2002): The climatology of sea breezes on Sardinia, *Int. J. Climatol.*, **22**, 917–932.

Grisogono, B., Ström, L. and Tjernström, M. (1998): Small-scale variability in the coastal atmospheric boundary layer, *Bound.-Lay. Meteorol.*, **88**, 23–46.

Iwasaki, H. (2004): Diurnal variation of precipitable water and convective activity with dual maxima in summer season around Mt. Tanigawa in the Northern Kanto District, Japan, *J. Meteorol. Soc. Jpn.*, **82**, 805–816.

Klaić, Z. B., Pasarić, Z. and Tudor, M. (2009): On the interplay between sea-land breezes and etesian winds over the central Adriatic, *J. Marine Syst.*, **78**, S101–S118, DOI: 10.1016/j.jmarsys.2009.01.016, 2009.

Kondo, H. (1990): A numerical experiment of the »extended sea breeze« over the Kanto Plain, *J. Meteorol. Soc. Jpn.*, **68**, 419–434.

Laird, N. F., Kristovich, D. A. R., Liang, X.-Z., Arritt, R. W. and Labas, K. (2001): Lake Michigan lake breezes: Climatology, local forcing, and synoptic environment, *J. Appl. Meteorol.*, **40**, 409–424, DOI: 10.1007/s10546-007-9185-6.

Lukšić, I. (1989): Diurnal winds in Senj, *Geofizika*, **6**, 59–74. (in Croatian)

Makjanić, B. (1958): *Sea/land breezes: contribution to the mathematical theory and sea/land breeze analysis along Adriatic coast*, Ph.D. thesis, University of Zagreb, Faculty of Science, Zagreb, Croatia, 146 pp.

Miller, S. T. K., Keim, B. D., Talbot, R. W. and Mao, H. (2003): Sea breeze: Structure, forecasting, and impacts, *Rev. Geophys.*, **41**, 1–31.

Mikuš, P., Prtenjak, M. T. and Strelec Mahović, N. (2012): Analysis of the convective activity and its synoptic background over Croatia, *Atmos. Res.,* **104–105**, 139–153 DOI: 10.1016/j.atmosres.2011.09.016.

Nicholls, M. E., Pielke, R. A. and Cotton, W. R. (1991): A two-dimensional numerical investigation of the interaction between sea breezes and deep convection over the Florida peninsula, *Mon. Wea. Rev.*, **119**, 298–323.

Nitis, T., Kitsiou, D., Klaić, Z. B., Prtenjak, M. T. and Moussiopoulos, N. (2005): The effects of basic flow and topography on the development of the sea breeze over a complex coastal environment, *Q. J. Roy. Meteor. Soc.*, **131**, 305–328.

Pielke, R. A. (1974): A three-dimensional numerical model of the sea breezes over south Florida, *Mon. Wea. Rev.*, **102**, 115–139.

Pielke, R. A. and Mahrer, Y. (1978): Verification analysis of the University of Virginia three-dimensional mesoscale model prediction over south Florida for 1 July 1973, *Mon. Wea. Rev.*, **106**, 1568–1589.

Pielke, R. A. (1991): The predictability of sea-breeze generated thunderstorms, *Atmosfera*, **4**, 65–78.

Prtenjak, M. T., Grisogono, B. and Nitis, T. (2006): Shallow mesoscale flows at the north-eastern Adriatic coast, *Q. J. Roy. Meteor. Soc.*, **132**, 2191–2216.

Prtenjak, M. T. and Grisogono, B. (2007): Sea/land breezes climatological characteristics along the northestern Adriatic coast, *Theor. Appl. Climatol.*, **90**, 201–215. DOI: 10.1007/s00704-006-0286-9.

Prtenjak, M. T., Pasarić, Z., Orlić, M. and Grisogono, B. (2008): Rotation of sea/land breezes along the northeastern Adriatic coast, *Ann. Geophys.*, **26**, 1711–1724.

Prtenjak, M. T., Viher, M. and Jurković, J. (2010): Sea/land breeze development during a summer bora event along the north-eastern Adriatic coast, *Q. J. Roy. Meteor. Soc.*, **136**, 1554–1571. doi: 10.1002/qj.649.

Sano, T. and Tsuboki, K. (2006): Structure and evolution of a cumulonimbus cloud developed over a mountain slope with the arrival of sea breeze in summer, *J. Meteorol. Soc. Jpn.*, **84**, 613–640.

Simpson, J. E. (1994): *Sea breeze and local winds*. Cambridge University Press, 234 pp.

Wilson, J. W. and Megenhardt, D. L. (1997): Thunderstorm initiation, organization, and lifetime associated with Florida boundary layer convergence lines, *Mon. Wea. Rev*., **125**, 1507–1525.

Yuter, S. E. and Houze, R. A. Jr. (1995): Three-dimensional kinematic and microphysical evolution of Florida cumulonimbus. Part I: Spatial distribution of updrafts, downdrafts and precipitation, *Mon. Wea. Rev*., **123**, 1921–1940.

SAŽETAK

Veza između plitke termalne cirkulacije zraka i kumulonimbusa nad Sjevernim Jadranom

Karmen Babić, Petra Mikuš i Maja Telišman Prtenjak

Cilj je ove studije odrediti vezu između pojave smorca i kumulonimbusa (Cb) nad Istrom. Pritom se koriste raspoloživa standardna prizemna mjerenja, kao što su prizemni vjetar, prizemna temperatura zraka, površinska temperatura mora i naoblaka na dvije postaje (zračna luka Pula i Pazin) te satelitske slike. Analiza koja se vršila za ljetne mjesece (od lipnja do rujna) u razdoblju 1997.–2006. je pokazala da je Cb razvoj učestaliji u određenim meteorološkim uvjetima. Oni su bili: (i) brzina smorca na postaji zračna luka Pula u intervalu od 3–5 m s⁻¹, (ii) maksimalna temperaturna razlika između kopna i mora oko 4 °C u blizini zračne luke Pula i (iii) maksimalna temperatura zraka u Pazinu u intervalu od 25 do 31 °C. U usporedbi s drugim analiziranim danima, kopnenjak je bio nešto slabiji i temperatura zraka je bila viša onih dana kada je registrirana istovremena pojava SB i Cb nad Istrom. Dnevni razvoj oblaka je pokazao da se Cb oblak uobičajeno razvija nad Pazinom između 13 and 14 h po srednjeeuropskom vremenu. Kumulusni oblaci povrh i ispred SB fronte, (koja je indikator prodiranja morskog zraka u unutrašnjost), prethodili su Cb razvoju. Satelitske slike u razdoblju 2000.–2006. dobivene geostacionarnim satelitima Meteosat 7 i 8 su pokazale prostornu razdiobu i vremensku evoluciju 30 odabranih slučajeva Cb razvoja. Uočena su dva karakteristična područja nastanka Cb: sjeverni i jugoistočni dio Istre. Oblaci Cb tipa se uobičajeno formiraju između 11 i 13 h po srednjeeuropskom vremenu, traju od 3 do 5 sati te nestaju između 15 i 17 h po srednjeeuropskom vremenu.

Ključne riječi: smorac/kopnenjak, Istra, zona konvergencije, satelitske slike, indeks smorca

Corresponding authors' address: Karmen Babić and Maja Telišman Prtenjak, University of Zagreb, Faculty of Science, Department of Geophysics, Andrija Mohorovičić Geophysical Institute, Horvatovac 95, HR-10000 Zagreb, Croatia, tel. +385 (0)1 4605 900, fax: +385 (0)1 4680 331, babick@gfz.hr; telisman@gfz.hr